GENERALIZED EMPIRICAL LAWS OF STARTING DISCONTINUITY DYNAMICS ASSOCIATED WITH THE STARTUP OF UNDEREXPANDED JETS

A. V. Emel'yanov and A. V. Eremin

UDC 533.6;534.220

The process of formation of an underexpanded jet is accompanied by the formation of complex gas-dynamic structures — shock waves and rarefaction waves, contact surfaces. The geometry, amplitudes, and dynamics of these structures depend on a large number of governing parameters such as the stagnation and underexpansion parameters, the composition of the gas, the dimensionality of the flow, and the characteristic dimensions of the nozzle. The motion of the starting discontinuities associated with jet startup has been investigated in numerous experimental [1-4] and theoretical [5-8] studies. In [4, 7, 9] attempts were made to introduce generalizing parameters suitable for modeling the process of jet formation in different flow regimes. The starting points were the generalizing parameters and similarity criteria developed for the flows in steady supersonic jets and, moreover, in the theory of point explosions [10]. The next step was to introduce additional criteria to take into account the unsteady processes in the jet startup stage [1, 2, 8]. Because of the approximations of the analytic models employed and the limited number of experimental regimes investigated the published data do not make it possible to formulate universal similarity criteria which could be used to describe the dynamics of the starting gas-dynamic structures in the form of equations that do not depend on the above-mentioned parameters of the flow.

The aim of the present study was to analyze a large number of experimental data on the motion of the starting discontinuities along the jet axis and to obtain single relations describing their dynamics over a broad range of the governing parameters. Numerous experiments were carried out on two-dimensional (plane) supersonic jets flowing from a sonic slit nozzle into various model gases (Ar, N_2, CO_2) over a broad range of temperatures, stagnation pressures, and underexpansion ratios. We also analyzed the previous experimental data [1-3] obtained for both pane and axisymmetric jets over the range of underexpansion ratios from 10 to 10^8.

In those experimental regimes in which the jet flowed into a space with back pressure, i.e., when the pressure of the background gas $p_\infty \geq 0.1$–1 Pa, an unsteady gas-dynamic structure, which, apart from the expanding-gas front itself, includes the primary shock traveling through the background gas and the secondary shock that matches the pressure in the gas with the pressure in the ambient space, is formed in the starting flow. Propagating upstream at velocities less than the flow velocity, this secondary wave gradually drifts away from the section near the nozzle exit where it was formed towards its steady-state position. In a number of experiments not one but two secondary waves were observed [11] together with certain irregularities in the dynamics of all the above-mentioned starting discontinuities.

Below, the motion of the principal gas-dynamic discontinuities (expanding-gas front, primary and secondary shocks) along the jet axis is analyzed within the framework of second-degree polynomials corresponding to the model proposed in [1, 7].

The experiments were carried out on an apparatus consisting of a combination of a shock tube and a vacuum chamber [11]. The gas flowed from a slit nozzle with half-width $r_* = 1.15$ mm and length $d = 40$ mm in the end face of a shock tube connected to a vacuum chamber in which a special adapter designed to ensure the two-dimensionality of the flow was mounted. The process was recorded by the schlieren method using a standard IAB-451 instrument and a spark light source whose intensity, giving an exposure of about 1 μsec made it possible to record the flow pattern in the pulsed jet to half-scale. The large-frame records allowed the details of the structure to be analyzed and the coordinates of the surfaces of discontinuity to be accurately determined relative to the nozzle exit. For framewise recording the random error in determining the wave velocities was about 1%.

Moscow. Translated from Zhurnal Prikladnoi Mekhaniki i Tekhnicheskoi Fiziki, No. 5, pp. 22-26, September-October, 1991. Original article submitted May 10, 1990.

0021-8944/91/3205-0665$12.50

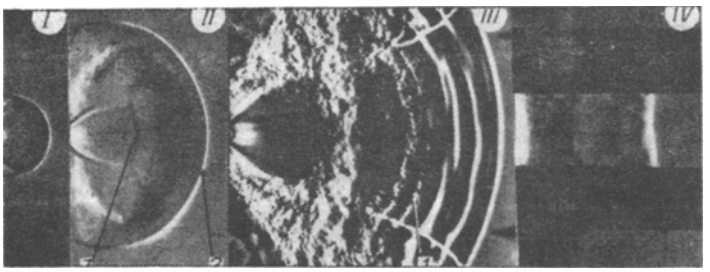

Fig. 1

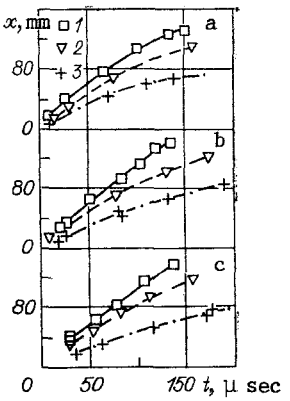

Fig. 2

In the experiments the Mach numbers of the incident shock wave in the shock tube were M = 8-3, which corresponded to T_0 = 3000-1000 K in CO_2, T_0 = 5000-1500 K in N_2, and T_0 = 13,000-2500 K in Ar. The initial underexpansion ratio was varied over the range $N = p_0/p_\infty$ = 1000–50.

Schlieren photos of the process were obtained in two planes for different stages of the flow, starting 7-10 μsec from the onset of flow and ending with the flow pattern corresponding to 300 μsec. The maximum time was limited by the size of the two-dimensional adapter (200 mm). A comparison of the flow patterns for nitrogen, argon, and carbon dioxide jets shows that, in general, the flow development is similar. Figure 1 reproduces examples of shadowgraphs in which the dynamics of the starting discontinuities in various flow regimes are clearly visible: I corresponds to nitrogen with $p_\infty = 8\cdot10^2$ Pa and M = 6.54, II to argon with $p_\infty = 5.6\cdot10^3$ Pa and M = 5.45, III to carbon dioxide with $p_\infty = 5.3\ 10^4$ Pa and M = 3.44, and IV to carbon dioxide with $p_\infty = 1.07 \times 10^3$ Pa and M = 7.47 at right angles to the major axis of the nozzle. In all stages the expanding-gas front 1 with its characteristic vortex structure is clearly visible and in the background gas it is possible to observe the primary shock 2 which in the immediate vicinity of the nozzle edge stands off from the expanding-gas front and travels at a velocity greater than that of the front. When $p_\infty > 1.33\cdot10^3$ Pa a secondary wave 3 appears in the expanding gas, again in the immediate vicinity of the nozzle exit. At lower pressures it is not always observed. It is apparent that the jet angle increases on transition from Ar to N_2 and CO_2.

Figure 2a-c show the motion of the expanding-gas front in Ar, N_2, and CO_2 respectively for various ambient pressures p_∞. Points 1-3 represent the experimental data for $p_\infty = 8\cdot10^2$; $5.6\cdot10^3$; $5.3\cdot10^4$ Pa, and the curves equations of motion of the form $t = ax + bx^2$ obtained from a least-squares analysis of the experimental results. The slowing of the front, which increases with increase in back pressure, is clearly visible. Thus, for the lowest back pressure $p_\infty = 8\cdot10^2$ Pa in N_2 and CO_2 on the flow interval recorded the motion of the expanding-gas front is almost linear, without slowing, but when $p_\infty = 5.3\cdot10^4$ Pa in N_2 and CO_2 the velocity of the front more than halves on the interval from 20 to 100 mm from the nozzle exit.

In [1] a study of the laws of motion of the expanding-gas front for an axisymmetric nozzle made it possible to generalize the experimental data for Ar and N_2 in the similarity coordinates $\psi = x/(r_*\sqrt{N})$, $\theta = tu_m/(r_*\sqrt{N})$ ($u_m = 2c_0/(\gamma - 1)$ is the maximum velocity of unsteady flow into a vacuum) and to obtain empirical equations of motion of the front in these coordinates for Ar and N_2.

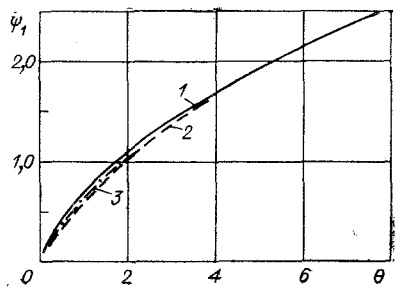

Fig. 3

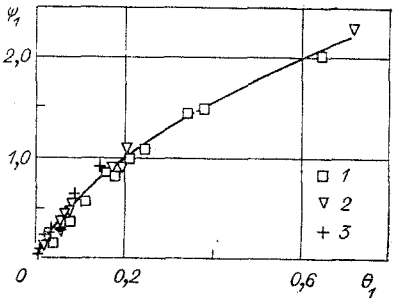

Fig. 4

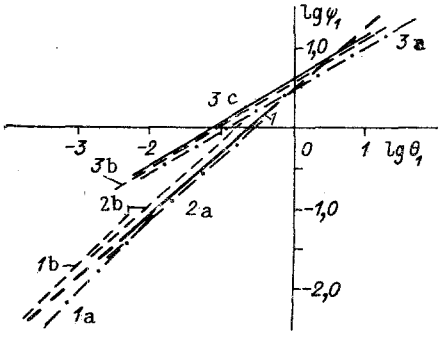

Fig. 5

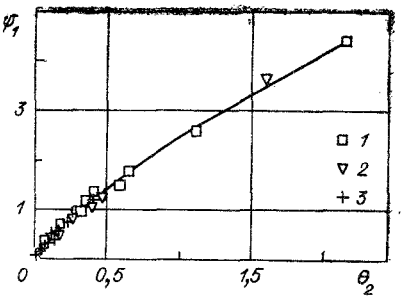

Fig. 6

The results of our experiments on the dynamics of the expanding-gas front, represented in the similar coordinates $\psi = x/(r_* N^{1/\alpha})$ and $\theta = tu_m/(r_* N^{1/\alpha})$ (where the exponent $1/\alpha$ takes into account the dimensionality of the flow: $\alpha = 1$ for a two-dimensional jet, $\alpha = 2$ for an axisymmetric jet), whether for different flow regimes in the same gas or for similar flow regimes in different gases, cannot be generalized. The discrepancy between the data for Ar and CO_2 reaches 100%. Thus, in order to find the generalized equation of motion of the expanding-gas front it was necessary to continue the search for similarity criteria reflecting different flow regimes and the physical properties of different gases.

As a first step, we obtained a generalization in each gas for various flow regimes. The flow regimes differ with respect to the ratio N and temperature. Since N already enters into the coodinate ψ and no generalization can be obtained from varying its exponent, it is necessary to supplement ψ with a multiplier that takes the temperature factor into account. In [7] this multiplier entered into the similarity coordinates in the form $(T_0/T_\infty)^{-0.5}$; however in the case of our experiments this did not lead to generalization.

In analyzing the results, it was noted that generalization is obtained in each gas when the exponent of the temperature factor entering into the ψ coordinate has different values for each gas. By comparing them we were able to write a general expression for the component in the form $(\gamma - 1)/2$. Thus the ψ coordinate, represented in the form:

$$\psi_1 = \left[x/(r_* N^{1/\alpha})\right](T_0/T_\infty)^{(\gamma-1)/2},$$

generalizes all the flow regimes obtained in each gas. Figure 3 shows the generalization in Ar for various flow regimes (curves 1-3 are for N = 380, 190, and 57, respectively) in the coordinates ψ_1 and θ. The generalization picture is similar for N_2 and CO_2. In these coordinates the discrepancy between the data obtained in different regimes does not exceed 8%, but the difference between them in different gases reaches 300%.

In the second step, it was necessary to supplement the coordinate with a multiplier that differed for each gas. An analysis of the motion of the expanding gas front along the flow axis showed that when the velocity of unsteady flow into a vacuum ($u_m = 2c_0/(\gamma - 1)$) or the steady flow velocity ($u_S = \sqrt{2/(\gamma - 1)}\cdot c_0$) was used in the coordinate, generalization in different gases could not be obtained. However, when the multiplier $((\gamma - 1)/2)^2$ is introduced into the θ coordinate it is possible to generalize the motion of the front for all the gases investigated. Thus, θ should be written as

$$\theta_1 = \frac{t}{r_* N^{1/\alpha}} \frac{\gamma - 1}{2} c_0.$$

Figure 4 gives the experimental points 1-3 for Ar, N_2, and CO_2 in different flow regimes and the generalizing relation in the coordinates ψ_1 and θ_1. In these coordinates the generalized equation of motion of the expanding-gas front takes the form:

$$\theta_1 = 0{,}1\psi_1 + 0{,}1\psi_1^2; \tag{1}$$

it is correct to within about 10% for a two-dimensional jet in Ar, N_2, and CO_2 when ψ_1 = 0.05–2.3.

The results of our experiments (the straight line 1) and the previously obtained relations for the motion of the expanding-gas front in axisymmetric jets are compared in the coordinates log ψ_1 and log θ_1 in Fig. 5: 1a corresponds to Ar and 1b to N_2 for $N = 10^8$, $T_0/T_\infty = 1$ [1]; 2a corresponds to Ar and 2b to N_2 for $N = 10^6$, $T_0/T_\infty = 1$ [2]; 3a corresponds to Ar, 3b to N_2, and 3c to CO_2 for N = 50-100, T_0/T_∞ = 6-12 [3]. From a comparison with all the previously obtained results for the motion of an expanding-gas front it is clear that the equation obtained in the similarity parameters ψ_1 and θ_1 most fully describes the motion of the front. It can be recommended for describing the motion of an expanding-gas jet front in the unsteady stage of flow.

The experimental results on the dynamics of the secondary shock propagating in the expanding gas were subjected to a similar analysis. The experimental data can be satisfactorily generalized in the similarity coordinates θ_1 and ψ_1. The equation of motion of the secondary wave takes the form:

$$\theta_1 = -0{,}07\psi_1 + 0{,}8\psi_1^2, \tag{2}$$

where ψ_1 varies over the interval 0.25-2.3. The negative coefficient of the linear term reflects the fact that the secondary wave is formed not at the edge of the nozzle but at a certain distance from it ($\psi_1 \geq 0.1$). The coefficient of ψ_1^2 has a larger value than in equation (1), which reflects the considerable slowing of the secondary wave and its lagging behind the expanding-gas front.

When the data on the motion of the primary wave in the background gas were analyzed for Ar, N_2, and CO_2 generalization in the coordinates ψ_1 and θ_1 was not obtained, whereas in each gas individually the experimental results were well generalized by the coordinate ψ_1. In varying the coordinate θ_1 it is necessary to take into account the fact that the primary wave moves in a background gas having a constant initial temperature for all the regimes investigated: T_0 = 300 K. In the analysis of the experimental data this determined the weaker dependence of the θ_1 coordinate on the multiplier $(\gamma - 1)/2$, i.e., as distinct from θ_1 the data are generalized by introducing $((\gamma - 1)/2)^{3/2}$. Thus, the θ coordinate takes the form

$$\theta_2 = \frac{t}{r_* N^{1/\alpha}} \sqrt{\frac{\gamma - 1}{2}} c_0.$$

In this case the experimental data on the motion of the primary wave are described by the equation

$$\theta_2 = 0{,}11\psi_1 + 0{,}09\psi_1^2.$$

In Fig. 6 it is shown that the data (points 1-3 for Ar, N_2, and CO_2) are generalized (to within about 10%) in the coordinates θ_2, ψ_1.

Thus, the empirical relations obtained can be recommended for describing the dynamics of the starting discontinuities when underexpanded jets are started up in different flow regimes.

LITERATURE CITED

1. A. V. Eremin, V. A. Kochnev, A. A. Kulikovskii, and I. M. Naboko, "Unsteady processes associated with the startup of underexpanded jets," Zh. Prikl. Mekh. Tekh. Fiz., No. 1 (1978).
2. A. V. Emel'yanov, A. V. Eremin, and I. M. Naboko, "Local electron-beam investigations of the pulsed-jet formation process," in: Proc. 9th All-Union Conf. Rarefied Gas Dynamics [in Russian], Vol. 3, Izd-vo Ural'sk Univ., Sverdlovsk (1988).

3. V. A. Belavin, V. V. Golub, I. M. Naboko, and A. I. Opara, "Investigation of the unsteady flow structure of a shock-heated gas get," Zh. Prikl. Mekh. Tekh. Fiz., No. 5 (1973).
4. V. V. Volchkov, A. V. Ivanov, N. I. Kislyakov, et al., "Low-density jets expanding from a sonic nozzle with large pressure differences," Zh. Prikl. Mekh. Tekh. Fiz., No. 2 (1973).
5. V. N. Gusev, "Supersonic nozzle startup," Inzh. Zh., No. 1 (1961).
6. G. A. Simons, "The large-time behavior of a steady spherical source expanding into an arbitrary ambient gas," AIAA Paper No. 70, New York (1970).
7. S. F. Chekmarev, "Unsteady radial expansion of gas into a fluid-filled space from a suddenly switched-on steady source," Zh. Prikl. Mekh. Tekh. Fiz., No. 1 (1975).
8. S. F. Chekmarev and N. V. Stankus, "Gasdynamic model and similarity relation for the startup of supersonic nozzles and jets," Zh. Tekh. Fiz., 54, No. 8 (1984).
9. V. G. Dulov and G. A. Luk'yanov, "Gasdynamics of Outflow Processes [in Russian], Nauka, Novosibirsk (1984).
10. V. P. Korobeinikov, N. S. Mel'nikova, and E. V. Ryazanov, "Theory of Point Explosion [in Russian], Fizmatgiz, Moscow (1961).
11. V. V. Golub and A. M. Shul'meister, "Starting shock waves and vortex structures associated with jet formation," Izv. Akad. Nauk SSSR, Mekh. Zhidk. Gaza, No. 5 (1988).

SHOCK WAVES IN POLYDISPERSE BUBBLY MEDIA WITH DISSIPATION

S. L. Gavrilyuk and S. A. Fil'ko

UDC 532.529.5

The shock wave structure in a bubbly liquid with a discrete bubble size distribution function (at each point in space there are bubbles of M different radii) is investigated. In the coordinate system moving with the wave the equations of motion reduce to a dynamical system in 2M-dimensional phase space. For an arbitrary finite M the existence, uniqueness and stability of the corresponding structure are proved. Stability is understood in the sense of satisfaction of the Cemplen theorem at the shock wave, treated within the framework of the equilibrium model as a strong discontinuity.

1. Mathematical Model

For low bubble concentrations the equations of motion of a polydisperse bubbly medium with a incompressible carrier phase have the form [1, 2]:

$$v_t - u_q = 0; \tag{1.1}$$

$$u_t + p_q = 0; \tag{1.2}$$

$$R_i R_{itt} + 3R_{it}^2/2 = \left(p_2^i(R_i) - p\right)/\rho_l - 4\mu_i R_{it}/(\rho_l R_i); \tag{1.3}$$

$$e_{2it} = 0,\ n_{it} = 0,\ i = 1, \ldots, M. \tag{1.4}$$

Here, t is time, q is the mass Lagrangian coordinate, u is velocity, v is the specific volume of the mixture, p is the pressure in the liquid, R_i are the radii of the bubbles, i denotes the corresponding bubble fraction (kind), $p_2^i(R_i)$ is the pressure in a bubble of the i-th kind, ρ_ℓ is the density of the liquid (constant), μ_i are the effective dynamic viscosity coefficients [3, Part 1, pp. 125, 126], c_{2i} are the mass bubble concentrations, and n_i is the number of bubbles per unit mass of mixture. As shown in [3], in liquids with vicosities of the same order as the viscosity of water the damping of fairly large bubbles is mainly determined by thermal dissipation. Since the heat transfer from the bubble to the liquid is

Novosibirsk. Translated from Zhurnal Prikladnoi Mekhaniki i Tekhnicheskoi Fiziki, No. 5, pp. 26-34, September-October, 1991. Original article submitted January 22, 1990.

